$F'_{\mathbf{h}}$. Then the structure factor is given by

$$F_{\mathbf{h}} = F'_{\mathbf{h}}[1 + \exp \pi i(h_1 + h_2 + h_3) + \exp \pi i(h_1 + h_2 + h_4) + \exp \pi i(h_3 + h_4)]. \quad (A10)$$

Here the second, third and fourth terms correspond to the contribution from the summation over the elements of three cosets $(\mathrm{E}|\frac{1}{2}, \frac{1}{2}, 0)\mathrm{G}_0$, $(\mathrm{E}|\frac{1}{2}, \frac{1}{2}, 0, \frac{1}{2})\mathrm{G}_0$ and $(\mathrm{E}|0, 0, \frac{1}{2}, \frac{1}{2})\mathrm{G}_0$. The last factor in (A10) gives the extinction rules $h_1 + h_2 + h_3 = 2n$, $h_1 + h_2 + h_4 = 2n$, $h_3 + h_4 = 2n$ and for the reflections which fulfill these conditions, this takes 4. Therefore the structure factor is calculated only by taking into account the symmetry operator in $\mathrm{G}_0$. This is analogous to the situation in the usual three-dimensional centered lattice.

### References


AXE, J. D. (1980). *Phys. Rev. B*, **21**, 4181–4190.

BOWN, M. G. & GAY, P. (1958). *Z. Kristallogr.* **111**, 1–14.

FLEET, S. G., CHANDRASEKHAR, S. & MEGAW, H. D. (1966). *Acta Cryst.* **21**, 782–801.

GROVE, T. L., FERRY, J. M. & SPEAR, F. S. (1983). *Am. Mineral.* **68**, 41–59.

HAMILTON, W. C. (1965). *Acta Cryst.* **18**, 502–510.

HORST, W., TAGAI, T., KOREKAWA, M. & JAGODZINSKI, H. (1981). *Z. Kristallogr.* **157**, 233–250.

JANNER, A. & JANSSEN, T. (1977). *Phys. Rev. B*, **15**, 643–658.

KITAMURA, M. & MORIMOTO, N. (1975). *Proc. Jpn Acad.* **51**, 419–424.

KITAMURA, M. & MORIMOTO, N. (1977). *Phys. Chem. Miner.* **1**, 199–212.

KOREKAWA, M. & JAGODZINSKI, H. (1967). *Schweiz. Mineral. Petrogr. Mitt.* **47**, 269–278.

MEGAW, H. D. (1960). *Proc. R. Soc. (London) Ser. A*, **259**, 159–183.

MORIMOTO, N. (1979). *AIP Conf. Proc.* No. 53, pp. 299–310.

MORIMOTO, N., NAKAJIMA, Y. & KITAMURA, M. (1975). *Proc. Jpn Acad.* **51**, 725–728.

NAKAJIMA, Y., MORIMOTO, N. & KITAMURA, M. (1977). *Phys. Chem. Mineral.* **1**, 213–225.

OVERHAUSER, A. W. (1971). *Phys. Rev. B*, **3**, 3173–3182.

RIBBE, P. H. & GIBBS, G. V. (1969). *Am. Mineral.* **54**, 85–94.

RIBBE, P. H., MEGAW, H. D. & TAYLOR, W. H. (1969). *Acta Cryst.* B**25**, 1503–1518.

SMITH, J. V. (1983). Abstr. 3rd NATO Advanced Study, Institute of Feldspars. *Feldspars and Their Paragenesis*, 32.

TAGAI, T. (1980). *Die Untersuchung der modulierten Kristallstrukturen des intermediaren Plagioklases* $An_{52}$. Thesis, Frankfurt Univ.

TAGAI, T., JOSWIG, W. & KOREKAWA, M. (1980). *Z. Kristallogr.* **151**, 77–89.

TOMAN, K. & FRUEH, A. J. (1973). *Z. Kristallogr.* **138**, 337–342.

TOMAN, K. & FRUEH, A. J. (1976). *Acta Cryst.* B**32**, 526–538.

WENK, H., JOSWIG, W., TAGAI, T., KOREKAWA, M. & SMITH, K. B. (1980). *Am. Mineral.* **65**, 81–95.

WOLFF, P. M. DE (1974). *Acta Cryst.* A**30**, 777–785.

WOLFF, P. M. DE, JANSSEN, T. & JANNER, A. (1981). *Acta Cryst.* A**37**, 625–636.

YAMAMOTO, A. (1982*a*). *Acta Cryst.* A**38**, 87–92.

YAMAMOTO, A. (1982*b*). *Acta Cryst.* B**38**, 1446–1451.

YAMAMOTO, A. & INOUE, Z. (1981). *Acta Cryst.* A**37**, 838–842.

YAMAMOTO, A. & NAKAZAWA, H. (1982). *Acta Cryst.* A**38**, 79–86.


*Acta Cryst.* (1984). B**40**, 237–244

# A High-Resolution Electron Microscopy Study of Disorder in Two Types of Rutile-Related Crystallographic-Shear Phases


BY L. C. OTERO-DIAZ* AND B. G. HYDE

*Research School of Chemistry, Australian National University, GPO Box 4, Canberra, ACT Australia*


(*Received* 10 *October* 1983; *accepted* 3 *January* 1984)


## Abstract

Two specimens were studied: rutile that had been melted in an argon-arc furnace, and therefore slightly reduced, and a $V_2O_3$-doped $TiO_2$ of nominal composition $(V, Ti)O_{\sim 1.875}$ which had been quenched from 1873 K. Both were examined at the atomic-resolution level. The former contained only a few areas with crystallographic-shear planes, and these were roughly parallel to $(1\bar{3}2)_r$, and appeared quite 'thick' in projection along $[1\bar{1}1]_r$. (The subscript $r$ indicates the rutile subcell.) The latter contained a $(253)_r$ crystallographic-shear structure with $n \approx 23$. In both cases the crystallographic-shear planes showed variations in orientation. A tentative explanation of the observed phenomena is proposed. [Crystal data for the first specimen: $a = 4{\cdot}5940\,(1)$, $c = 2{\cdot}9600\,(1)$ Å, $V = 62{\cdot}4688\,(2)$ Å$^3$.]


## 1. Introduction

The titanium oxide ('reduced rutile') system has been extensively studied for half a century, and is established as a prototype case in which there are sequences of ordered structures with definite but 'grotesque' stoichiometries. From $TiO_{1.750}$ to $TiO_{1.889}$ the


* Present addresses: Departamento de Química Inorgánica, Facultad de Ciencias Químicas, Universidad Complutense, Madrid-3, and Instituto de Química Inorgánica Elhuyar CSIC, Serrano 113, Madrid-6, Spain.


0108-7681/84/030237-08$01.50

sequence is $Ti_nO_{2n-1}$, $4 \leq n \leq 9$; the structures being derived from a rutile parent by crystallographic shear (CS) at regular intervals on planes parallel to $(121)_r$. The different stoichiometries are attained by different spacings between the CS planes (CSP's). From $TiO_{1.938}$ to $TiO_{1.98}$ a similar sequence has $16 \leq n \leq 40$ or 50, but the CSP's are now parallel to $(132)_r$. In the intervening composition range, $1.889 < O/Ti \leq 1.938$, the sequence is $Ti_nO_{2n-p}$ ($n$ and $p$ both integers, with $p > 1$), but the CSP orientation varies monotonically between $(121)_r$ and $(132)_r$. In all cases the displacement vector across the CSP is $\mathbf{R} \approx \frac{1}{2}[0\bar{1}1]_r$ (Bursill & Hyde 1972).

More recent results show that, contrary to earlier assertions, at equilibrium at high temperatures there is a range of composition, $TiO_{2-\delta}$ with $\delta \leq 0.03$, which approximates to a 'homogeneous solid solution' (Baumard, Panis & Anthony, 1977). In this phase region CSP's are absent from samples *rapidly* quenched from high temperatures; though not from those cooled slowly or previously subjected to mechanical deformation (Blanchin, Faisant, Picard, Ezzo & Fontaine, 1980).

The most recent results indicate that, in some instances at least, the 'CSP's' are no longer planar: they are continuous surfaces with small-scale (tens of Å) variations in orientation (Bursill, Blanchin & Smith, 1982; Wood, Bursill & Smith, 1983). We too have observed this; and describe our observations here. Such a phenomenon had been suspected (Philp, 1972); definite proof awaited the advent of the modern, high-resolution electron microscope.

The present study involves two preparations. The first was an (argon) arc-melted sample of rutile (*i.e.* slightly reduced and very rapidly quenched). The second was a reacted mixture of $V_2O_3 + TiO_2$ annealed at 1873 K and then quenched. (We may note that 'rutiles' are reduced by, in effect, adding $Ti_2O_3$; but similar phenomena are also produced by adding oxides of other, lower-valent cations such as $Fe_2O_3$, $V_2O_3$, $Cr_2O_3$, $Ga_2O_3$ *etc.*)

## 2. Experimental methods

### 2.1. *Sample preparation*

2.1.1. *Sample* (1). A 1 g pressed pellet of high-purity rutile powder (99·999%, Koch-Light) was melted in an argon-arc furnace for 30 s. The temperature was probably above 2273 K [*cf.* $T_m = 2123(25)$ K for rutile: Brauer & Littke (1960)]. The resulting button was dark blue in colour; characteristic of reduced rutile.

2.1.2. *Sample* (2). This had a nominal composition of $(V, Ti)O_{1.875}$, and was prepared by heating a mixture of $V_2O_3$ and $TiO_2$ (in a mole ratio of 1:6) in a sealed, evacuated, silica tube at 1373 K for 3 d, after which the tube was slowly cooled to room temperature. A portion of this product (in a sealed Pt capsule) was then annealed at 1873 K for 2 h, and quenched by dropping into cold water.

Table 1. *Unit-cell parameters for various rutile specimens*

| $a$ (Å) | $c$ (Å) | $V$ (Å$^3$) | O/Ti | Reference |
|---|---|---|---|---|
| 4·5940 (1) | 2·9600 (1) | 62·4688 (2) | ? | Present work |
| 4·594 (3) | 2·959 (2) | 62·45 (6) | 2·000 | Baur (1956) |
| 4·59366 (2) | 2·958682 (8) | 62·4332 (3) | 2·000 | Abrahams & Bernstein (1971) |
| 4·5845 (1) | 2·9533 (1) | 62·071 (3) | 1·984 (7) | Shintani, Sato & Saito (1975) |

### 2.2. *Examination by X-ray diffraction*

A Guinier–Hägg focusing camera (XDC-700) was used to obtain powder patterns, using monochromatic Cu $K\alpha_1$ radiation ($\lambda = 1.5405981$ Å) and 6N purity Si powder as an internal standard [$a = 5.4305$ (1) Å].

### 2.3. *Examination by electron microscopy/diffraction*

A JEOL 200 CX microscope, fitted with a top-entry goniometer (±10° of tilt) and $LaB_6$ filament, was used to obtain diffraction patterns and high-resolution images. The objective lens had $C_s = 1.2$ mm. Exposure times were ~2 s at a magnification of 550 000×. Selected crystals were ground under ethanol, and dispersed on Cu grids with holey-carbon support films. Crystal fragments projecting over holes in the carbon film were oriented into the $[1\bar{1}1]_r$ zone axis: the essential orientation. Through-focal series of images were recorded, using an objective aperture with $R = (1.5\ \text{Å})^{-1}$.

## 3. Results

### 3.1. *X-ray measurements*

3.1.1. *Sample* (1). The Guinier film only contained lines corresponding to the rutile structure; no additional lines were visible. Unit-cell parameters were calculated, and are compared with previously published values in Table 1. The differences are hardly significant, except for the last sample which is significantly reduced.

3.1.2. *Sample* (2). Not surprisingly, the Guinier films from this sample showed 'rutile' reflections split into doublets or triplets, plus many additional lines (Philp, 1972). We have not been able to index them unequivocally.

### 3.2. *Electron microscopy*

3.2.1. *Sample* (1). The majority of the crystal flakes examined gave a rutile-like diffraction pattern, and their images exhibited uniform contrast. Thus, in

these cases there was no indication of any type of extended defect such as CSP's. (Compare the X-ray results in § 3.1.1.)

On the other hand, a few of the flakes examined did contain planar defects. An example is given in Fig. 1, with the corresponding diffraction pattern (with the appropriate $[1\bar{1}1]_r$ zone axis) in Fig. 2. The latter contains short rows of weak extra reflections parallel to $\mathbf{g}(132)_r$, and centred on the strong reflections characteristic of the rutile (sub-) structure. These rows appear to consist of several coincident sets of superlattice reflections with different periodicities, and there are additional spots, particularly towards the boundaries of the zone, which probably correspond to similar superlattices in a twin orientation not in this zone. The $\mathbf{g}(132)_r$ periodicity corresponds to $n \geq 30$ $(132)_r$, *i.e.* $Ti_{30}O_{59} = TiO_{\sim 1.97}$.

Fig. 3 is a high-magnification, higher-resolution image obtained using an objective aperture with $R = (1{\cdot}5\ \text{Å})^{-1}$. {The black spots correspond to $[1\bar{1}1]$ rows of Ti atoms; and $(110)_r$, $(011)_r$ and $(101)_r$ planes of cations are clearly resolved.} It shows CSP's *approximately* parallel to $(132)_r$, but with considerable modifications. First there are (longitudinal) variations in orientation which lie between the two extremes of $(110)_r$ and $(011)_r$. [All CSP orientations are usually represented by $(hkl)_r = p(121)_r + q(011)_r$, so that $h = p$, $k = 2p + q$, $l = p + q$. But they are equally well decomposed to $p(110) + q'(011)_r$ with $q' = q + 1$.] Second, the dark regions at the CSP's are quite wide, up to ~6 Å or more. Except at the extreme (thin) edge of the crystal, this width does not vary very much with crystal thickness, *cf.* Fig. 4. This is certainly consistent with 'lateral' variations in orientation of the 'CSP's', *i.e.* that they are not uniformly parallel to the beam/$[1\bar{1}1]_r$ zone axis. Both these effects have recently been reported for slightly reduced rutile, $TiO_{1.9966}$ (Blanchin, Bursill, Hutchison & Gai, 1981) and $TiO_{1.9985}$ (Bursill, Blanchin & Smith, 1982), and for $Cr_2O_3$-doped rutile, $(Ti, Cr)O_{\sim 1.92}$ (Wood, Bursill & Smith, 1983), and discussed in considerable detail which we will not repeat. The lack of detailed contrast in the CSP regions may be understandable in terms of the short projected distances $d(Ti\cdots Ti)$ between cations. But the apparent width/thickness is much greater than has been reported previously.

There are considerable variations in the spacing of the CSP's, see Fig. 5 and preceding figures. In Fig. 5 it decreases almost monotonically from over 50 Å on the left to less than 30 Å on the right (corresponding to $n \approx 48$ and 29 respectively). Not unexpectedly, twinning of the CS structure is common (see especially Fig. 6), with regions in which the CSP's are tilted out of the zone, presumably to equivalent orientations such as $\sim(312)_r$, $(\bar{3}12)_r$, *etc.*

The CSP's appear to be single; not paired as sometimes reported (*e.g.* Blanchin *et al.*, 1981).

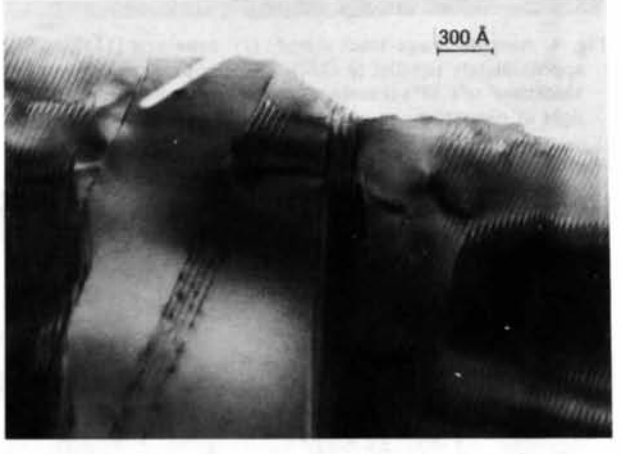


Fig. 1. An example of a not very common electron microscope image from sample (1) ('arc-melted rutile'). The planar features seen edge-on are $(132)_r$ CSP's. At the centre of the picture and at left and right centre other $\{132\}_r$ CSP's are tilted out of the $[1\bar{1}1]_r$ zone.

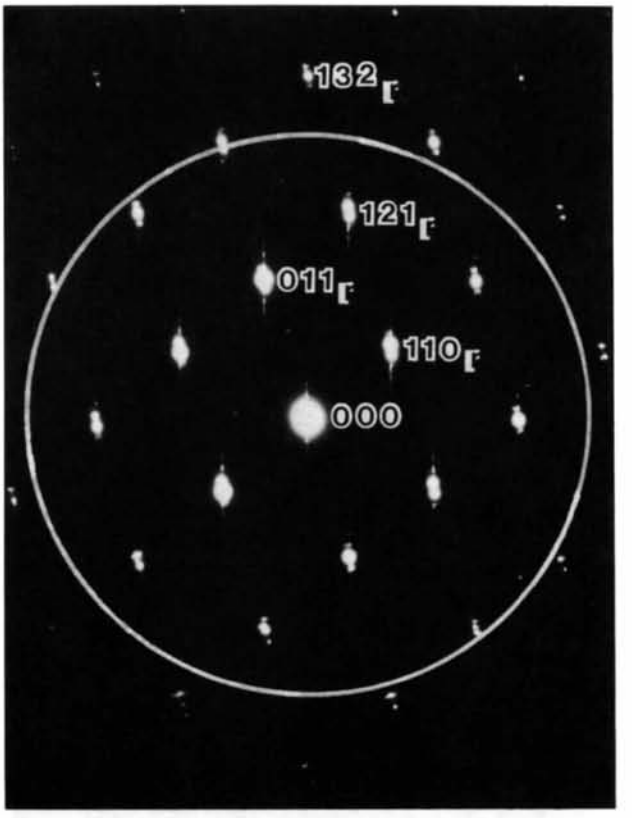


Fig. 2. $[1\bar{1}1]_r$ zone-axis diffraction pattern corresponding to the image in Fig. 1. The circle represents the objective aperture limiting the beams used to produce the image. The indices on the bright reflections are for the rutile subcell. Note the fine superstructure spots through these main reflections: they lie on rows approximately parallel to $\mathbf{g}(132)_r$. Additional spots are presumed to arise from groups of CSP's parallel to other $\{132\}_r$ orientations.

3.2.2. *Sample* (2). Fig. 7 is a $[1\bar{1}1]_r$ zone-axis diffraction pattern of the nominally $(V, Ti)O_{1\cdot875}$ specimen (quenched from 1873 K). It again contains short rows of superlattice reflections, but now parallel to $\mathbf{g}(253)_r$. [The measured angle between these rows and $\mathbf{g}(121)_r$ is $7\cdot0 \pm 0\cdot5°$ compared with the calculated value $(253)_r \wedge (121)_r = 7\cdot26°$.] Additional, very short rows are clearly not in the same zone, again suggesting equivalent (twin) CSP orientations. The direction of these rows is consistent with a superlattice parallel to $\mathbf{g}(\bar{5}23)_r$.

The main superlattice periodicity corresponds to $n \approx 23\,(253)_r$, *i.e.* $M_{23}O_{44} = MO_{1\cdot913}$, which is to be compared with the nominal $MO_{1\cdot875} \equiv n = 16\,(253)_r$.

Fig. 8 is the image corresponding to the diffraction pattern in Fig. 7. The lower-magnification part clearly shows cellular twinning on a fine scale, *e.g.* areas *A* and *B* in a direction parallel to the crystal edge. The *B* areas are clearly not appropriately oriented; their CSP's are not parallel to the beam. The insets are photographic enlargements of parts of the main print, and show the high resolution (clearly visible in the original print of the main figure). Where the CSP's are correctly oriented parallel to $[1\bar{1}1]$ they are seen to be approximately parallel to $(253)_r$. But, once again, there is some longitudinal variation about this mean orientation. (Note the reversed contrast here: white spots correspond to $[1\bar{1}1]_r$ rows of Ti atoms.)

A higher-magnification image from the same crystal is shown in Fig. 9. (The contrast is now reversed

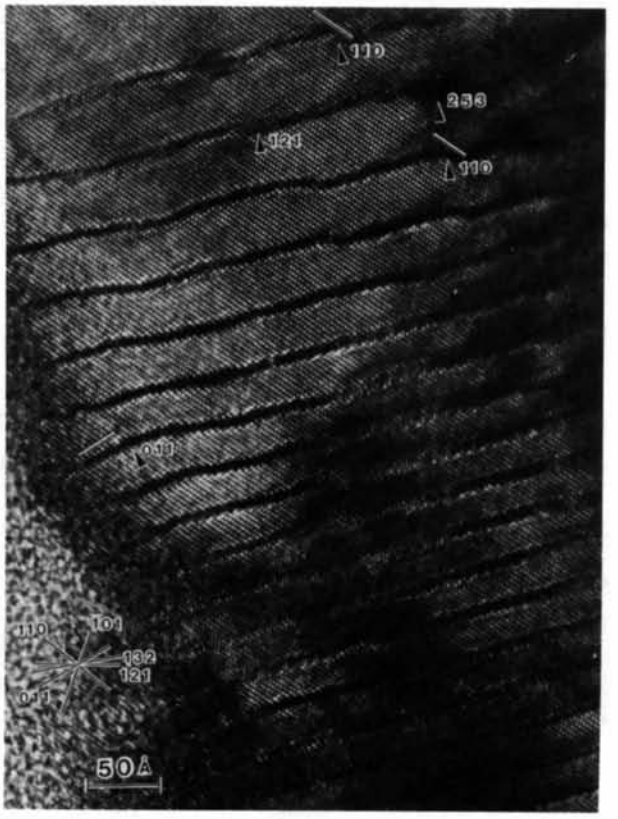


Fig. 3. A higher-magnification image from sample (1) (diffraction pattern as in Fig. 2). Black spots are $[1\bar{1}1]_r$ rows of Ti atoms. Notice that CSP's are approximately parallel to $(132)_r$, but that segments of them range between $(011)_r$ (centre left) and $(110)_r$ (top right).


Fig. 4. Another image from sample (1): zone axis $[1\bar{1}1]_r$; CSP's approximately parallel to $(132)_r$. Note approximately constant 'thickness' of CSP's (except at extreme edge of crystal – bottom right of picture).

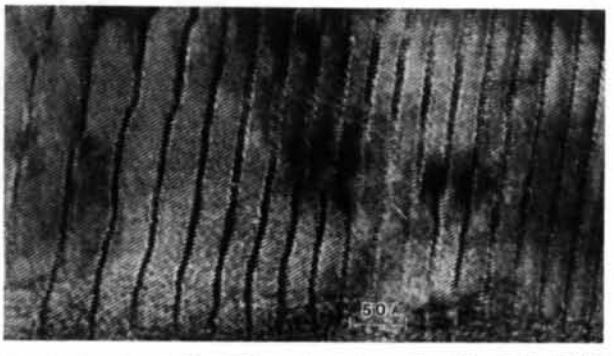


Fig. 5. Another $(132)_r$ CSP region of sample (1), with $d$(CSP) varying from ~52 Å at the left to ~23 Å at the right.

again: black blobs are Ti rows.) In contrast to sample 1 there is now very little lateral variation in CSP orientation (even in the thicker parts of the crystal, Fig. 8), although the longitudinal variations in orientation and variation in CSP spacing are still present.

Fig. 8 also exhibits marked boundaries approximately parallel to $(\bar{1}01)_r$. These appear to define the twin cells.

## 4. Discussion

The most striking result is fine-scale longitudinal variations in the orientations of the CSP's in both cases, as previously reported. In sample (1) the lateral variations (or 'thick' CSP's) are much greater than previously reported. We believe that there is a relevant factor operating here that has not been invoked in the previous discussions of such phenomena.

As already mentioned (§ 1), Baumard *et al.* (1977) and Blanchin *et al.* (1980) have produced a great deal of persuasive evidence that, at high temperatures (above ~1000 K), there is a *structurally* significant degree of non-stoichiometry in the homogeneous rutile phase, $TiO_{2-\delta}$. They have published a phase diagram of this region (Vrinat & Blanchin, 1981) which we reproduce in Fig. 10. It shows $\delta$ values increasing from ~0·003 at 1000 K to ~0·024 at ~1700 K. A similar trend appears for the upper limit of the CS phase region (O/Ti = $x \approx 1{\cdot}974$ at 1200 K, $\approx 1{\cdot}961$ at 1700 K). We have taken the liberty of roughly extrapolating their curves to higher temperatures (the broken lines in Fig. 10).

Measurement of the two-phase gap between these boundaries at four different temperatures in the range $1200 \leq T \leq 1720$ K gives $\Delta x = 0{\cdot}019$, 0·018, 0·016 and 0·014: a slow decrease with increasing temperature but, very approximately, a $\Delta x$ value that is constant in that temperature range. This leads us to speculate that the rutile-like slabs in the CS structures are also non-stoichiometric $TiO_{2-\delta}$, exactly as in 'rutile' itself. The extent of the non-stoichiometry for the latter is, from the diagram of Vrinat & Blanchin (1981), $\delta \approx 0{\cdot}01$ at 1323 K (1050 °C) and ~0·025 at 1723 K (1450 °C). Our sample (2) was annealed at 1873 K where our extrapolation indicates $\delta \approx 0{\cdot}04$. It may be

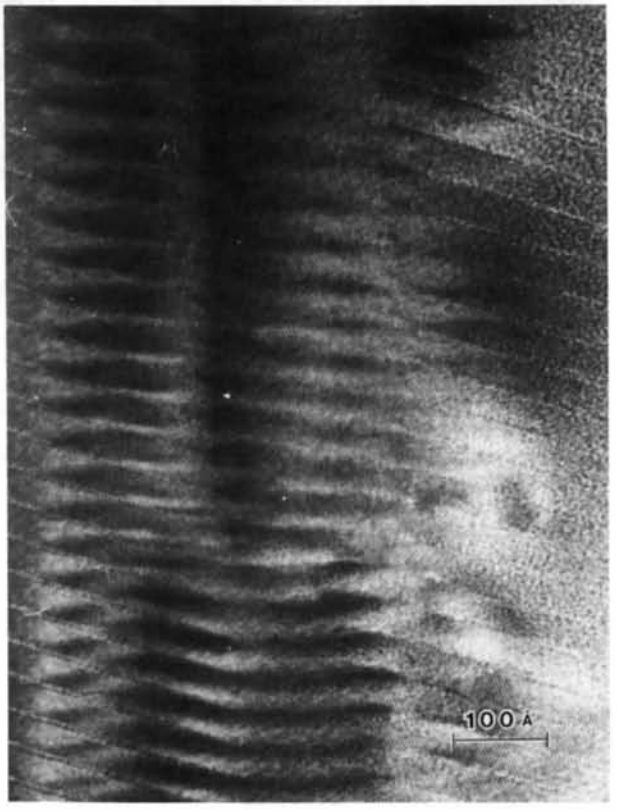


Fig. 6. CSP area of sample (1) showing repeated twinning of CSP's. At left and right the ~(132), CSP's are parallel to the electron beam (parallel to $[1\bar{1}1]_r$), but not in the centre where they are presumably parallel to some other $\{132\}_r$.

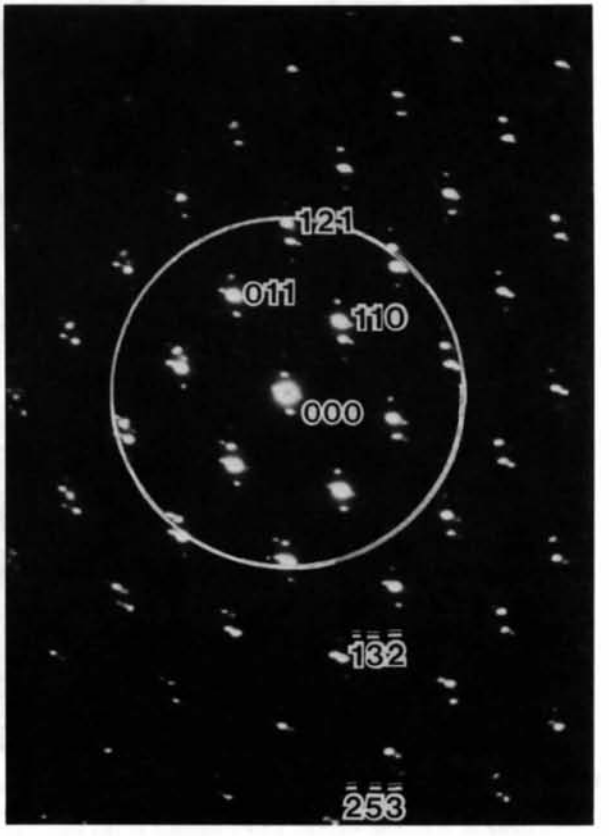


Fig. 7. $[1\bar{1}1]_r$ zone-axis diffraction pattern from sample (2), $(Ti, V)O_{\sim 1{\cdot}875}$, quenched from 1873 K. The main (almost vertical) superlattice rows are parallel to **g**(253), and the subsidiary ones (almost horizontal) are not in this zone, but probably parallel to $\mathbf{g}(\bar{5}23)_r$. The indices refer to the rutile subcell.

significant that the first value $\delta \approx 0{\cdot}04$ is remarkably close to the discrepancy between the nominal composition of our sample (2) and that deduced from the diffraction pattern in Fig. 7, *viz.* $x = 1{\cdot}875$ and $1{\cdot}913$ respectively – a difference $\Delta x = \delta' = 0{\cdot}038$.

A plausible alternative explanation is simply that sample (2) was oxidized during its 1873 K anneal (in a Pt tube sealed by welding its crimped ends). We are now examining this by further experiments. Nevertheless, the diagram in Fig. 10 clearly shows that, at high enough temperatures, $(132)_r$ CS structures transform to the rutile-like phase, $TiO_{2-\delta}$, with no change of composition; *i.e.* that samples characterized by electron microscopy/diffraction will *appear to oxidize* when annealed at high temperatures.

It has been proposed (Odier, Baumard, Panis & Anthony, 1975; Blanchin *et al.*, 1980) that the non-stoichiometry $\delta$ is accommodated (at least at temperatures in the range with which we are concerned here) by additional, 'interstitial' Ti atoms (not by a deficit in the O array). Bursill & Blanchin (1983) have proposed an elegant structural model for accommodating these extra Ti atoms which avoids the (structurally and energetically) unacceptable aspects of a simple interstitial Ti atom. At the same time they show that the defect is simply an element in the structure of all CSP's. An interstitial Ti atom ($Ti_i$) produces a $[100]_r$ column of three face-sharing $TiO_6$ octahedra ($Ti_3$). By one Ti atom jumping to an adjacent, empty octahedron this is converted to two adjacent *pairs* of face-sharing octahedra $(Ti)_2$:

$$3Ti_{Ti} + Ti_i \rightarrow Ti_{Ti} + (Ti)_3 \rightarrow 2(Ti)_2.$$

This last element is a basic structure unit in the corundum type (of $Ti_2O_3$) and all CS planes.

Such excess Ti atoms will tend, at lower temperatures, to precipitate out – by aggregating with each other (to form CSP's) or, particularly, with any suitable extended defects. These last may be dislocations – which accounts for the appearance of CSP's

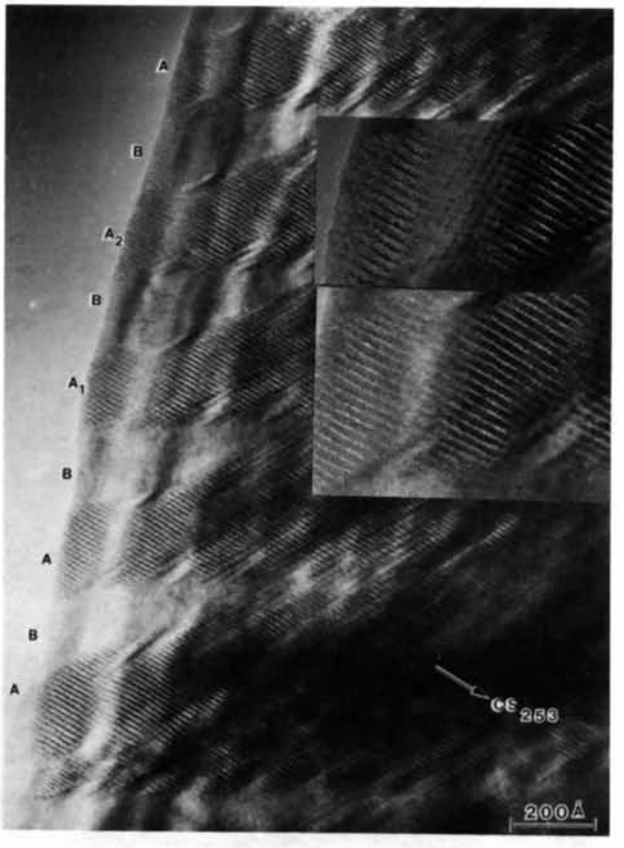


Fig. 8. A low-magnification image corresponding to the diffraction pattern in Fig. 7 (zone axis $[1\bar{1}1]_r$). Notice the cellular twins; only those at *A* having ~(253), CSP's parallel to the zone axis. Clearly there are four orientations – presumably equivalent {253}, – with two intersecting sets of composition planes running almost vertically and horizontally. The insets are two areas, $A_1$ and $A_2$, at higher magnification which reveal the high resolution in the main photograph. (Ti, V atoms rows parallel to $[1\bar{1}1]_r$ are white blobs.)

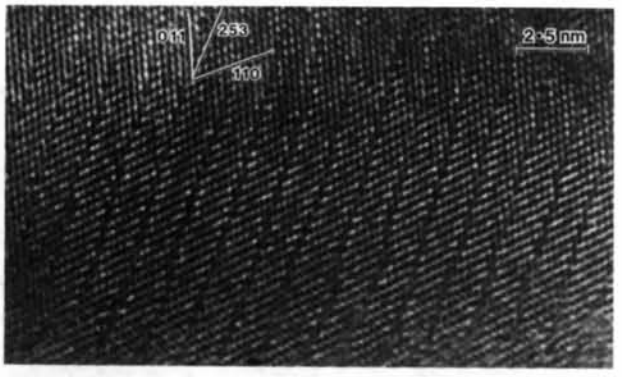


Fig. 9. A higher-magnification image of an area in the same crystal as in Figs. 7 and 8. (Cation rows are now black blobs.) There is still considerable longitudinal disorder, but now little lateral disorder or CSP 'thickening'. The CSP spacing is not regular. The thin edge of the crystal is just off the bottom of the print. The loss of CSP contrast at the top is due to a composition plane (not parallel to $[1\bar{1}1]_r$) located there.

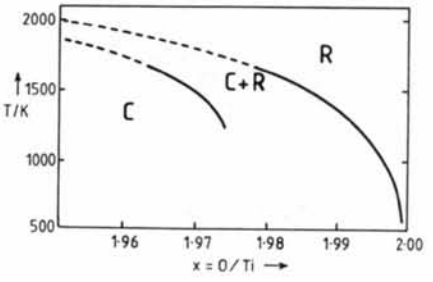


Fig. 10. Phase diagram for $TiO_x + O_2$ in the region $1{\cdot}96 \leq x \leq 2{\cdot}00$ after Vrinat & Blanchin (1981). The region *R* is non-stoichiometric rutile, $TiO_{2-\delta}$; the region *C* is that of the $(132)_r$ CS phases; $C + R$ is the diphasic (solid) region separating them.

in mechanically deformed (but not in undeformed), slightly reduced rutile, when rapidly quenched (Blanchin *et al.*, 1980) – or antiphase boundaries (APB's), $\frac{1}{2}[0\bar{1}1]_r(011)_r$. In the case of more heavily reduced rutile the features on which the extra Ti atoms precipitate will be CSP's, particularly the (stoichiometric) *A* steps of the type that generate $(011)_r$ APB's. In this way *A* steps will be converted to *C* steps (*cf.* Fig. 11, and Bursill & Hyde, 1972): $A + \mathrm{Ti} \rightarrow C$. As a result, the planar fault will 'swing': the extremes being $(011)_r \rightarrow (121)_r$; *i.e.* all *A* steps to all *C* steps.

In the case of sample (2) the mean CSP orientation is $(253)_r$, in which the proportion of $A:C$ steps is 1:2. The CSP's are very closely spaced [$d(\mathrm{CSP}) \approx$ 14 Å], which means that no extra Ti atom need diffuse more than ~10 Å to reach an *A* step. Very much larger displacements than this are readily achieved during even the most rapid quench (O'Keeffe, 1970). The apparent structure of sample (2) is $n \approx 23$ $(253)_r$. This corresponds to a unit cell with 23 Ti atoms and one *A* step and two *C* steps in the *perfect* structure. But, as deduced above, the real structure would (at temperature) also have $\delta \approx 0{\cdot}04$, which corresponds to an extra $0{\cdot}04/2 = 0{\cdot}02$ Ti atoms in the perfect structure; *i.e.* a total of 0·46 extra Ti atoms per unit cell. If all these extra Ti atoms precipitated on to the CSP during the quench (and none remained 'dissolved' in the rutile slabs between the CSP's, or escaped to the surface of the crystal), then about one half of the *A* steps would be changed to *C* steps, and the CSP orientation would ideally change from $(253)_r$ (=four *C* steps + two *A* steps in two unit cells) to ~$(5, 11, 6)_r$ (= five *C* steps + one *A* step in one unit cell). This is a 'swing' of ~4° on the average, but up to ~30° [$(011)_r \rightarrow (121)_r$] locally, since a uniform swing is unlikely because of the large diffusion distances

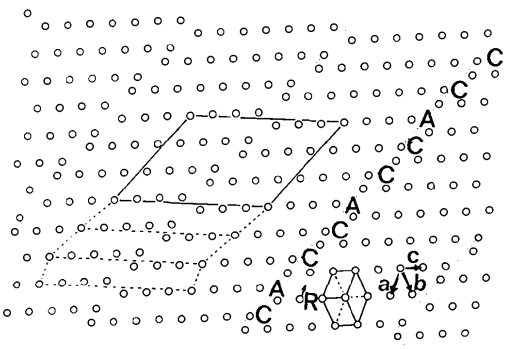


Fig. 11. The Ti-atom array in the $n = 23$ (253)$_r$ CS structure projected along $[1\bar{1}1]_r$. The CSP's and unit cell are shown, as well as a decomposition of the cell into one unit cell of $n = 7$ $(011)_r$ plus two unit cells of $n = 8$ $(121)_r$ according to

$$23\,(253)_r = 7\,(011)_r + 2\times[8\,(121)_r]$$

or

$$M_{23}O_{44}\,(253)_r = M_7O_{14}\,(011)_r + 2M_8O_{15}\,(121)_r.$$

required at large distances from the 'pivot'. Preferentially, segments of each CSP would swing; and the segments would be connected by new segments (approximately) parallel to $(011)_r$ (which is a *stoichiometric* planar fault). Swings of about this magnitude, over distances of the order of 100 Å, can be seen in Fig. 8.

Of course, this explanation still does not preclude the existence of longitudinal or lateral variations in CSP orientations at equilibrium at high temperature. It does suggest that in quenched samples these are likely to be less for (*a*) CSP's $(hkl)_r = p(121)_r + q(011)_r$ with a *higher* ratio $q/p$ (at a given stoichiometry) – because the proportion of $A/C$ steps is then higher, and (*b*) lower *n* values (*i.e.* lower stoichiometric ratios O/Ti) and the same $(hkl)_r$ – because now the number of extra Ti atoms per unit area of CSP is smaller (assuming, perhaps too naively, that the concentration of additional Ti in the rutile slabs is independent of the width of these slabs).

In these terms the case of sample (1) is, at the same time, more extreme and more difficult to speculate about. To consider it, there is one obvious question which is a logical outcome of the explanation just given for sample (2): this is, what is the result if the number of 'dissolved', additional Ti atoms is more than enough to convert all *A* steps to *C* steps? Sample (1) is extreme in exactly this way: the average CSP spacing is certainly much greater than in sample (2). (See Fig. 1; and also recall that most of the sample is free of CSP's.) This means that (per unit area of CSP) the available volume from which the additional Ti atoms can be collected is very much larger, and hence that the density of precipitated Ti atoms is very much larger also. This situation is accentuated by the fact that the preparation temperature is higher and $\delta$ therefore greater also (~0·06 compared with ~0·04; not a very great factor). The greater mean diffusion path required is not expected to limit these effects significantly. Hence we might expect that even though this sample has $(132)_r$ CSP [with a ratio $A:C$ steps of 1:1 instead of 1:2 for $(253)_r$ CSP in sample (2)] the number of *A* steps will be insufficient to accommodate all the Ti atoms precipitating on to the CSP during the quench.

When all the *A* steps are converted to *C*, the CSP orientation is $(121)_r$. We recall (*cf.* Fig. 4 of Bursill & Hyde, 1972) that the structure of this CSP is exactly that of a lamella of corundum type. So, it is not unreasonable to expect that the addition of still more Ti atoms will simply increase the thickness of the corundum-like layer parallel to $(121)_r$. Once again, it is not plausible that the whole area of a CSP will pivot as a rigid unit from $(132)_r$ to $(121)_r$. It is more likely that small segments will pivot and be connected *via* steps which may lie somewhere between $(011)_r$ APB's and $(132)_r$ CSP's – if the pivot is $[1\bar{1}1]_r$. This last condition is unlikely (*cf.* the twinning normally

present; see especially Fig. 6); and so the final, 'thick' corundum layer may well have lateral corrugations also. But the end result is a thin lamella of corundum-like $Ti_2O_3$ coherently intergrown with $TiO_{2-\delta}$ (where $\delta$ may be very small indeed, down to zero in regions close to CSP's). This, we suggest, is the explanation of the wide, dark bands at the CSP's in Figs. 4, 5 and 6.

We are grateful to Mr Peter Barlow for assisting with the electron microscopy. One of us (LCO-D) wishes to thank the Research School of Chemistry for a Visiting Fellowship which enabled this work to be completed.

### References

ABRAHAMS, S. C. & BERNSTEIN, J. L. (1971). *J. Chem. Phys.* **55**, 3206–3211.

BAUMARD, J. F., PANIS, D. & ANTHONY, A. M. (1977). *J. Solid State Chem.* **20**, 43–51.

BAUR, W. H. (1956). *Acta Cryst.* **9**, 515–520.

BLANCHIN, M. G., BURSILL, L. A., HUTCHISON, J. L. & GAI, P. L. (1981) *J. Phys. (Paris) Colloq.* **42**, C3, 95–112.

BLANCHIN, M. G., FAISANT, P., PICARD, C., EZZO, M. & FONTAINE, G. (1980). *Phys. Status Solidi A*, **60**, 357–364.

BRAUER, G. & LITTKE, W. (1960). *J. Inorg. Nucl. Chem.* **16**, 67–76.

BURSILL, L. A. & BLANCHIN, M. G. (1983). *J. Phys. (Paris) Lett.* **44**, L165–L170.

BURSILL, L. A., BLANCHIN, M. G. & SMITH, D. J. (1982). *Proc. R. Soc. London Ser. A*, **384**, 135–155.

BURSILL, L. A. & HYDE, B. G. (1972). *Progr. Solid State Chem.* **7**, 177–253.

ODIER, PH., BAUMARD, J. F., PANIS, D. & ANTHONY, A. M. (1975). *J. Solid State Chem.* **12**, 324–328.

O'KEEFFE, M. (1970). *The Chemistry of Extended Defects in Non-metallic Solids*, edited by L. EYRING & M. O'KEEFFE, pp. 624–625. Amsterdam: North-Holland.

PHILP, D. K. (1972). Thesis. Univ. of Western Australia.

SHINTANI, H., SATO, S. & SAITO, Y. (1975). *Acta Cryst.* B**31**, 1981–1982.

VRINAT, M. & BLANCHIN, M. G. (1981). *J. Phys. (Paris) Colloq.* **42**, C3, 79–94.

WOOD, G. J., BURSILL, L. A. & SMITH, D. J. (1983). *J. Microsc. (Oxford)*, **129**, 263–273.

*Acta Cryst.* (1984). B**40**, 244–249

# On Anharmonicity in Zinc and Cadmium

BY ELISABETH ROSSMANITH

*Mineralogisch–Petrographisches Institut der Universität Hamburg, D-2000 Hamburg 13, Grindelallee 48, Federal Republic of Germany*

(*Received* 16 *December* 1982; *accepted* 19 *January* 1984)

## Abstract

X-ray diffraction data on Zn [Rossmanith (1977). *Acta Cryst.* A**33**, 593–601] and Cd [Rossmanith (1978). *Acta Cryst.* A**34**, 497–500] have been reanalyzed using a temperature factor based on an anharmonic one-particle potential to fourth order for the atoms in the crystal. Because of the strong correlation of the harmonic parameters $\alpha_{20}$, $\beta_{00}$ and the anharmonic parameters $\alpha_{33}$, $\alpha_{40}$, $\beta_{20}$, $\gamma_{00}$, the harmonic parameters of Zn were calculated using an approximate model. It is shown that for one set of harmonic parameters the results for the anharmonic parameters are ambiguous, giving a distribution of compatible values for the fourth-order anharmonic parameters. To check the influence of systematic errors on the anharmonic parameters introduced into calculations by absorption and extinction correction the results for two Cd single-crystal samples are compared. For the third-order parameter $\alpha_{33}$, which rules the antisymmetric part of the thermal motion, comparable values are found for both Cd samples. The results on the fourth-order anharmonic parameters for the two Cd crystals are not consistent.

## Introduction

From their X-ray data on Zn Skelton & Katz (1968) evaluated the mean-square displacements $\langle u_a^2 \rangle$ and $\langle u_c^2 \rangle$ in the **a** and **c** directions of the crystal respectively. Comparing their results with calculated values of Barron & Munn (1967) in quasiharmonic approximation using thermodynamic data, they concluded that the high-temperature discrepancy in $\langle u_a^2 \rangle_T$ may be caused by constant-volume anharmonic effects, whereas $\langle u_c^2 \rangle_T$ is consistent with theoretical values.

The Mössbauer technique was used by Albanese, Deriu & Ghezzi (1976) to obtain the anharmonic contribution to the Debye–Waller factor of Zn for vibrations parallel to the *c* axis from the temperature dependence of integrated Bragg intensities. In partial disagreement with the results of Skelton & Katz (1968), they found an anharmonic contribution to the atomic vibration in the **c** direction, not consistent with predictions of quasiharmonic theory.

Merisalo & Larsen (1977) used elastic thermal neutron data from a single crystal of Zn measured at 295 K to estimate the anharmonicity of lattice vibrations, treating the crystal as a system of independent

0108-7681/84/030244-06$01.50 